Article

The Direct Alloying of Steel through Silicothermic Self-Reduction of Chromite Ore Utilizing Si-Containing Solid Waste

Yiliang Chen [1,2], Zhengliang Xue [1,2] and Shengqiang Song [1,2,*]

[1] The State Key Laboratory of Refractories and Metallurgy, Wuhan University of Science and Technology, Wuhan 430081, China; chenyiliang@wust.edu.cn (Y.C.); xuezhengliang@wust.edu.cn (Z.X.)
[2] Key Laboratory for Ferrous Metallurgy and Resources Utilization of Ministry of Education, Wuhan University of Science and Technology, Wuhan 430081, China
* Correspondence: songs@wust.edu.cn

Abstract: Organosilicon materials generate copious amounts of Si-containing solid waste during production, leading to severe environmental pollution and substantial resource squandering. In pursuit of the resource utilization of Si-containing solid waste, this study conducted experimental research on the direct alloying of molten steel through the silicothermic self-reduction of chromite ore using Si-containing solid waste as a reducing agent. Additionally, thermodynamic analysis was performed, employing the thermodynamic calculation software FactSage 8.2 (Thermfact Ltd., Montreal, QC, Canada and GTT-Technologies, Aachen, Germany), to examine the equilibrium reactions of the silicothermic reduction of chromite ore and the variations in the thermodynamic equilibrium compositions of slag and metal phases. The results indicate a reduction sequence for the reducible components in chromite ore as $Fe_2O_3 \rightarrow Cr_2O_3$. The introduction of CaO and Al_2O_3 into the silicothermic self-reduction compacts altered the forms of Fe and Cr oxides in equilibrium, significantly reducing the standard Gibbs free energy (ΔG^0) of the silicothermic reduction reaction. The initial slag melting point decreased from 1700 °C without the addition of CaO and Al_2O_3 to 1500 °C with the addition of CaO and Al_2O_3. Correspondingly, the slag viscosity at 1600 °C decreased from 134.1 Pa·s without CaO and Al_2O_3 addition to 1.81 Pa·s with CaO and Al_2O_3 addition. The addition of CaO and Al_2O_3 accelerated the reduction of Cr oxide in chromite ore and enhanced the recovery of Cr, consistent with the thermodynamic calculation results. In the process of steelmaking through the direct alloying of chromite ore silicothermic self-reduction compacts, the final recovery rate of Cr increased from 86.4% without CaO and Al_2O_3 addition to 95.4% with CaO and Al_2O_3 addition.

Keywords: Si-containing solid waste; chromite ore; silicothermic self-reduction; direct alloying; thermodynamics

1. Introduction

Organosilicon materials are predominantly polymeric structures with Si-O-Si as the main chain, renowned for their exceptional corrosion resistance, oxidation resistance, and high-temperature endurance. Consequently, they find widespread applications in aerospace, electronics, chemical and light industries, solar power generation, automotive and mechanical engineering, construction, agriculture, pharmaceuticals, and healthcare [1–5]. The fundamental raw materials for synthesizing organosilicon materials are organosilicon monomers. Approximately 90% of organosilicon monomers in the market are synthesized directly through the Rochow–Müller process, using chloromethane and industrial Si [6–8]. However, the production of organosilicon monomers results in a substantial generation of Si-containing solid waste, primarily composed of high-boiling-point

residues, unreacted Si powder, copper powder, and other constituents carried out by fluidized beds [9,10]. Disposing of or incinerating these solid wastes directly not only leads to heavy metal pollution in the soil and groundwater, including copper, zinc, and tin, but also generates strong acid mist and liquid during combustion, causing secondary environmental pollution. Most importantly, it results in the significant wastage of silicon resources [7].

Therefore, the recycling of Si-containing solid waste generated during the production of organosilicon monomers has become an urgent issue in the organosilicon production industry. Consequently, some scholars have conducted research on the recycling of Si-containing solid waste through laboratory experiments. Wang et al. [11] effectively converted by-products such as low-boiling-point residues and methyltrichlorosilane produced by the Rochow–Müller process into high-value dimethyldichlorosilane using [BMIM]Cl-nAlCl$_3$ ionic liquid catalysts. Yu et al. [12] synthesized a novel Si/C anode composite material by utilizing Si powder extracted from solid Si waste generated in organosilicon production, combined with graphite and amorphous carbon. This approach demonstrated the feasibility of enhancing the commercial graphite anode of lithium-ion batteries using low-cost Si particles from industrial solid Si waste. Lu et al. [13] successfully prepared a series of MnO$_x$-promoted Ni catalysts with Al$_2$O$_3$-modified Si waste contact bodies as carriers, using the deposition–precipitation method for CO methanation. The catalyst exhibited excellent catalytic performance as well as a higher resistance to coking and sintering. Liu et al. [14] developed a simple and effective method to recover copper from solid waste generated from the preparation of organosilicon by the Rochow–Müller process, preparing efficient multi-component Cu-Cu$_2$O-CuO catalysts which can be reused for the Rochow–Müller process. The final copper recovery rate reached 96.4%, providing an effective pathway for the recovery of valuable metals. Guo et al. [15] also effectively extracted copper from Si-containing solid wastes by direct leaching with hydrogen peroxide and established the leaching kinetics. Cai et al. [16] proposed an optimized removal method combining low-temperature oxidative roasting and mixed acid leaching, with up to 99% of removal of Cl, Ca, and Fe, and greater than 94% of removal of Al and Ti in the solid wastes, which provided a feasible solution for the recovery of silicon resources.

The aforementioned studies have achieved a certain degree of recycling of Si-containing solid waste through various experimental methods. However, due to factors such as high costs and challenging process control conditions, the large-scale recycling of Si from Si-containing solid waste has not yet been realized. Si is a highly reducible element and is typically used as a reducing agent and deoxidizer in the steelmaking process. Some scholars have studied the reduction of oxides by the silicothermic method. Salina et al. [17] investigated the effects of basicity $w(CaO)/w(SiO_2)$ and ferro-silico-nickel dosage on the amount of Cr reduction and metal and slag chemical compositions in chromite ore based on the thermodynamic software of HSC Chemistry 6.12. The simulation results showed that increasing the slag basicity and increasing the dosage of ferro-silico-nickel can increase the reduction of Cr. In addition, Salina et al. [18,19] performed thermodynamic simulations of the silicothermic reduction processes of Cr, Fe, Mn, and Ni in multicomponent CaO-SiO$_2$-Cr$_2$O$_3$-FeO-MgO-MnO-Al$_2$O$_3$ and CaO-SiO$_2$-MgO-Al$_2$O$_3$-FeO-NiO-P$_2$O$_5$ multicomponent oxide systems. The thermodynamic possibilities for the reduction of Cr, Fe, Mn, and Ni in oxide systems were demonstrated. The yield of the metals increased with the increase in Si concentration in the reducing agent ferrosilicon. Heo et al. [20,21] investigated the effect of temperature and ferrosilicon addition on the behavior of the silicothermic reduction of MnO. The results showed that the recovery of Mn is thermodynamically proportional to the Si activity in the alloy melt, and the higher the temperature, the more favorable the reduction of MnO.

In light of this, this study takes pre-treated Si-containing solid waste, after impurity removal, as a reducing agent. It is mixed with chromite ore powder, compressed into silicothermic self-reduction compacts, and utilized in the direct alloying of molten steel in a converter, replacing the use of high-carbon ferrochromium for steel alloying. This approach

explores a novel pathway for the resource utilization of Si-containing solid waste generated in the preparation of organosilicon.

2. Materials and Methods

2.1. Raw Materials

The experimental raw materials comprise Si-containing solid waste obtained through pre-treatment operations such as washing and steam distillation, South African chromite ore, industrial pure iron (purity $\geq$ 99.9%), and chemical reagents CaO (purity $\geq$ 98%) and Al_2O_3 (purity $\geq$ 99%). Chemical composition analysis of Si-containing solid waste and chromite ore is performed using X-ray fluorescence spectroscopy (XRF, Thermo Scientific, ARL 9900, Waltham, MA, USA). The mass fractions of C and S in the Si-containing solid waste are determined using an infrared carbon–sulfur analyzer (LECO, CS-996, St. Joseph, MI, USA). The specific chemical compositions of the Si-containing solid waste and chromite ore are presented in Tables 1 and 2, respectively.

Table 1. Typical chemical composition of Si-containing solid waste (Wt.%).

Si	Fe	O	Cl	Cu	C	Al	Ti	Ca	P	Zr	V	Mn
68.56	9.52	7.90	4.29	3.39	2.60	1.25	1.05	0.64	0.14	0.13	0.13	0.11

Table 2. Typical chemical composition of chromite ore (Wt.%).

| Cr_2O_3	Fe_2O_3	Al_2O_3	MgO	SiO_2	CaO
46.02	26.10	13.60	10.25	0.98	0.28

As evident from Table 1, the main components of the Si-containing solid waste are Si, with traces of Fe, O, Cl, Cu, and other elements. Phase analysis of the Si-containing solid waste and chromite ore is conducted using X-ray diffraction (XRD, X'Pert Pro, Bruker, Ettlingen, Germany), as shown in Figure 1. Figure 1 reveals that the primary phase in the Si-containing solid waste is elemental Si, along with impurities such as ferrosilicon and cuprous chloride. In contrast, Cr in the chromite ore is present in spinel, indicating a single phase composition [22].
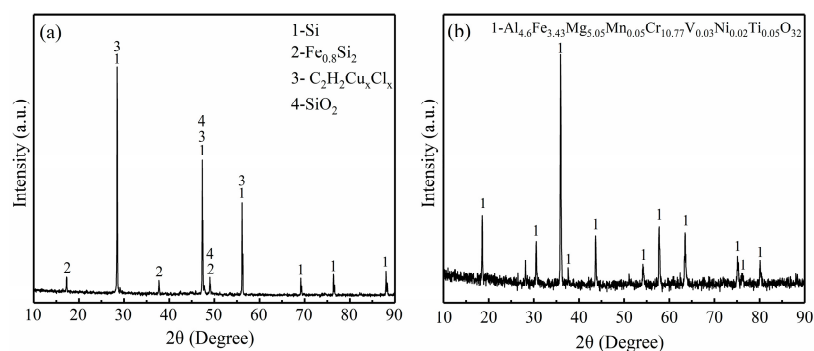
Figure 1. The X-ray diffraction pattern: (**a**) Si-containing solid waste; (**b**) chromite ore.

Microscopic morphology and energy spectrum analysis of Si-containing solid waste are carried out using a scanning electron microscope (SEM, ZEISS ASIN EVO10, Carl Zeiss AG, Jena, Germany) equipped with an energy-dispersive spectrometer (EDS, X-Max 80, Oxford Instruments, Abingdon, UK), as depicted in Figure 2a. From the figure, it is evident that the Si-containing solid waste is primarily composed of two types of particles. One type consists of particles with a higher Si content, typically enveloped in an oxide film on the surface and exhibiting unevenly sized pits. These pits result from the erosion of the catalyst during the preparation of organosilicon monomers through the Rochow–Müller

process [23,24]. The second type is a mixture of various elements, including Si, O, Fe, Cl, Cu, etc., with a lower Si content. Simultaneously, particle size distribution of the Si-containing solid waste is analyzed using an MS2000 laser particle size analyzer (Malvern Panalytical, Worcestershire, UK), as shown in Figure 2b. The average particle size of the Si-containing solid waste is measured to be 50.1 μm.
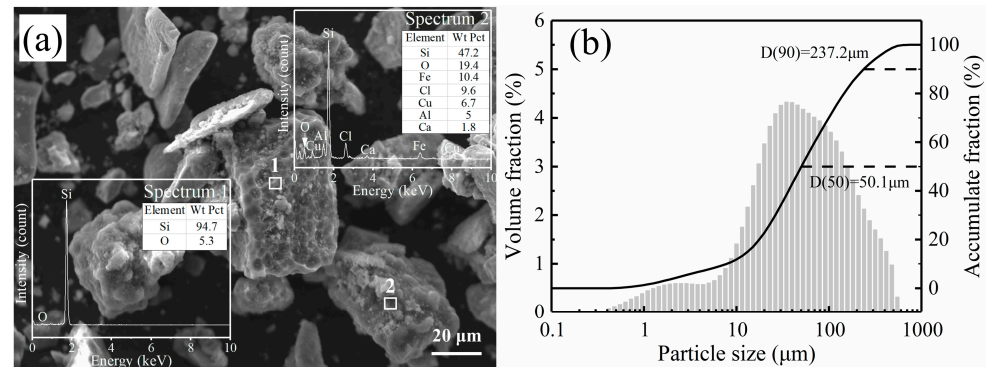
Figure 2. SEM analyses and particle size distribution of Si-containing solid waste: (**a**) SEM analyses; (**b**) particle size distribution.

2.2. Experimental Research Methodologies

2.2.1. Preparation of Silicothermic Self-Reduction Compacts

Prior to commencing the smelting process, the Si-containing solid waste and chromite ore are meticulously comminuted in a sample pulverizer. The objective is to augment the specific surface area of the reducing agent and chromite ore, facilitating thorough interaction between chromite ore and the reducing agent. Subsequently, the milled composite is moistened with water and molded at a pressure of 25 MPa to yield φ15 mm silicothermic self-reduction compacts. These compacts can be categorized into two types: one solely comprising pressed chromite ore and Si-containing solid waste (S1, without CaO, Al_2O_3 addition), and the other incorporating not only chromite ore and Si-containing solid waste but also supplemented with CaO and Al_2O_3 reagents (S2, with CaO, Al_2O_3 addition). Refer to Table 3 for specific compositional details. According to the content of oxygen in Cr_2O_3 and Fe_2O_3 in chromite ore, the ratio between chromite ore and Si-containing solid waste is determined by material proportioning according to the Si/O molar ratio of 0.8. In order to obtain higher Cr yields as much as possible, the addition of Si is in excess. Post molding, the silicothermic self-reduction compacts are placed in a forced-air drying chamber and subjected to a temperature of 120 °C for 2 h to ensure adequate dryness for later use.

Table 3. The raw material ratio of silicothermic self-reduction compacts (Wt.%).

| Components	Chromite Ore	Si-Containing Solid Waste	Al_2O_3	CaO
S1	62.4	37.6	-	-
S2	34.7	21.0	16.6	27.7

2.2.2. Direct Alloying Experiment

The direct alloying experiment of molten steel is conducted in the CY-SP35-VIM temperature-controlled high-frequency induction furnace, as depicted in Figure 3. The graphite crucible is placed inside the quartz tube and heated by the induced current generated by the induction coil, and the temperature is monitored by the B-type thermocouple at the bottom of the graphite crucible. Initially, a MgO crucible containing industrial pure iron is placed inside the graphite crucible. Under a high-purity argon atmosphere (99.999%) and a flow rate of 0.25 L·min^{-1}, the temperature is incrementally raised at a rate of 25 °C·min^{-1}.

Once the temperature reaches 1600 °C, silicothermic self-reduction compacts are introduced into the melt through a top alumina feeding tube.
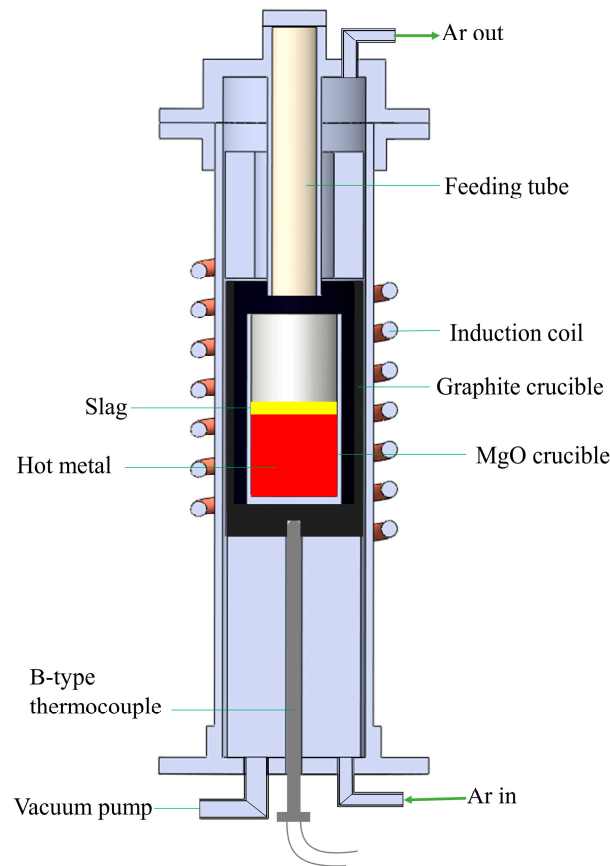
Figure 3. Schematic of high-frequency induction furnace setup.

Sampling operations are executed for the first two tests (Test 1 and Test 2), as illustrated in Figure 4. Upon reaching 1600 °C, silicothermic self-reduction compacts are added to the molten pool. The addition of silicothermic self-reduction compacts elicits a vigorous reaction, accompanied by flames near the feeding port. Following the completion of the reaction (approximately 1 min), the first sample (T1A1 and T2A1) is extracted using a 4 mm diameter quartz tube, followed by subsequent samples at intervals of 5 min or 10 min, and numbered sequentially. After sampling, the molten steel is cooled to room temperature at a rate of 30 °C·min^{-1}, yielding the final samples after direct alloying.
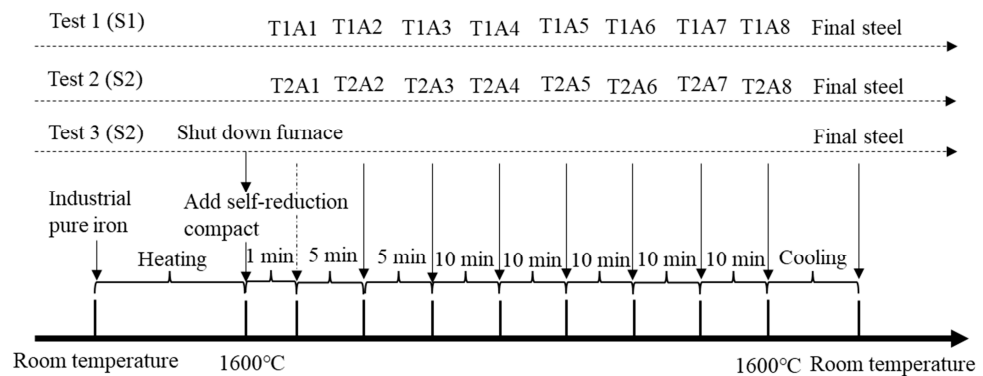
Figure 4. Schematic for silicothermic self-reduction compacts addition and sampling process.

Another set of experiments (Test 3) involves immediately shutting down the heating power upon introducing silicothermic self-reduction compacts with CaO, Al_2O_3 addition and allowing the furnace to cool to room temperature. The purpose of Test 3 is to observe the morphology and analyze the energy spectrum of the cooled slag sample through scanning electron microscopy, determine the initial phase composition and chemical composition when the self-reduction compacts are added to the surface of the steel, determine the degree of reduction of chromite ore in the early stage, and explore the reaction mechanism of silicothermic self-reduction. The mass fraction changes of Cr and Si in the process samples are determined using inductively coupled plasma atomic emission spectroscopy (ICP-AES, ThermoiCAP6000, Thermo Fisher Scientific, Waltham, MA, USA), and the final recovery rate of Cr is calculated using Equation (1) after performing XRF chemical composition analysis on the final slag.

$$\eta = \frac{\Sigma m_i w_i}{m_R w_R} \times 100 Pct \tag{1}$$

where η represents the recovery rate of Cr; m_i denotes the final mass of the steel sample; w_i is the final mass fraction of Cr in the steel sample; m_R is the mass of the self-reduction compacts; and w_R is the mass fraction of Cr in the self-reduction compacts.

## 3. Results and Discussion

3.1. Thermodynamic Analysis

Assuming that only Fe_2O_3 and Cr_2O_3 are reducible components in chromite ore, thermodynamic analysis of the Si reduction of Fe_2O_3 and Cr_2O_3 in chromite ore was conducted. Using FactSage 8.2 software (with databases FactPS, FToxid, and FTmisc), the standard Gibbs free energy (ΔG^0) of various reduction reactions was calculated within the temperature range of 400 to 1800 °C, as depicted in Figure 5. The calculations reveal that, when Si serves as the reducing agent, reduction reactions can occur in the temperature range of 400 to 1600 °C, all exhibiting strongly exothermic characteristics. Furthermore, based on the ΔG^0 of the reduction reactions, the reduction sequence is $Fe_2O_3 \rightarrow Cr_2O_3$. In the presence of CaO and Al_2O_3, the ΔG^0 of the reduction reactions is significantly reduced. Thermodynamically, the addition of CaO and Al_2O_3 facilitates the reduction of Cr_2O_3 in chromite ore, with CaO exerting a stronger influence. Additionally, the figure includes calculations of the ΔG^0 for the reduction reactions of Cr_2O_3 using Al and C as reducing agents. The variation in ΔG^0 indicates that Al exhibits the highest reduction capability, followed by Si, while C has the least within 1600 °C. However, considering cost, carbon is the preferred reducing agent in alloy smelting and steelmaking processes [25,26]. Therefore, utilizing Si-containing solid waste as a reducing agent for chromite ore reduction in the direct alloying of molten steel not only transforms waste into a valuable resource but also eliminates the need for smelting chromite alloy, thereby reducing costs, saving energy, and minimizing environmental pollution.

Furthermore, thermodynamic equilibrium analysis of the Si reduction of oxide components in chromite ore was conducted. Based on the principle of minimizing the Gibbs free energy, the relationship between the equilibrium quantities of oxides and metals in silicothermic self-reduction compacts and the molar quantity of Si was calculated at a constant temperature of 1600 °C using the "Equilib" module of FactSage 8.2 software (with databases FactPS, FToxid, and FTmisc), as depicted in Figure 6. From Figure 6, it is observed that in the absence of added Si and without CaO and Al_2O_3 addition, Fe and Cr in chromite ore primarily exist in the form of Fe_2O_3 and Cr_2O_3, respectively, with a small amount of $Al_2Fe_2O_6$. Upon the addition of CaO and Al_2O_3, Fe and Cr in chromite ore exist in the forms of calcium diiron oxide ($Ca_2Fe_2O_5$) and calcium chromate ($CaCr_2O_4$), respectively, indicating that the addition of CaO alters the forms of Fe and Cr. With the addition of Si, Fe oxides are initially reduced to FeO, which is further reduced to metallic Fe. When the Si addition is 0.024 mol, all FeO is reduced to metallic Fe, and at this point, Cr oxides begin to be reduced to metallic Cr. This corresponds to the earlier reduction of Fe_2O_3 compared to Cr_2O_3, as indicated by the ΔG^0 of the reduction reactions. In the absence of slag, Cr_2O_3

in chromite ore is directly reduced to metallic Cr, and by the time the Si addition reaches 0.068 mol, all Cr_2O_3 is completely reduced to metallic Cr. The Si added in this experiment is 0.1 mol, so it is enough to completely reduce Fe and Cr from chromite ore. In the case of silicothermic self-reduction compacts with CaO and Al_2O_3 addition, calcium chromate is not only reduced to metallic Cr but also generates intermediate products $(Ca_2Cr_3)Cr_{10}O_{20}$ and Cr_2O_3. After the complete reaction of calcium chromate, these oxides are then reduced to metallic Cr. Consequently, the addition of CaO can alter the forms of Fe and Cr during the reduction process, potentially affecting the final recovery rate. However, with a continuous increase in Si addition to 0.2 mol, the products of Fe and Cr converge, with Fe ultimately transforming into FeSi, and Cr gradually transforming into Cr_3Si and Cr_5Si_3, until the final product $CrSi_2$.
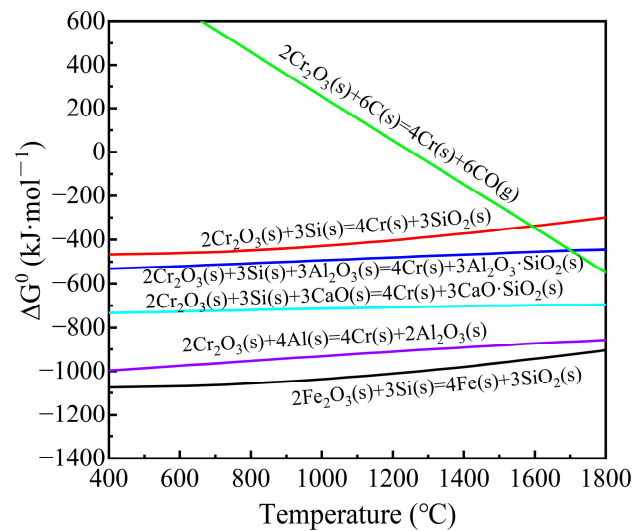

Figure 5. The relationship between standard Gibbs free energy (ΔG^0) and temperature for different reduction reactions.
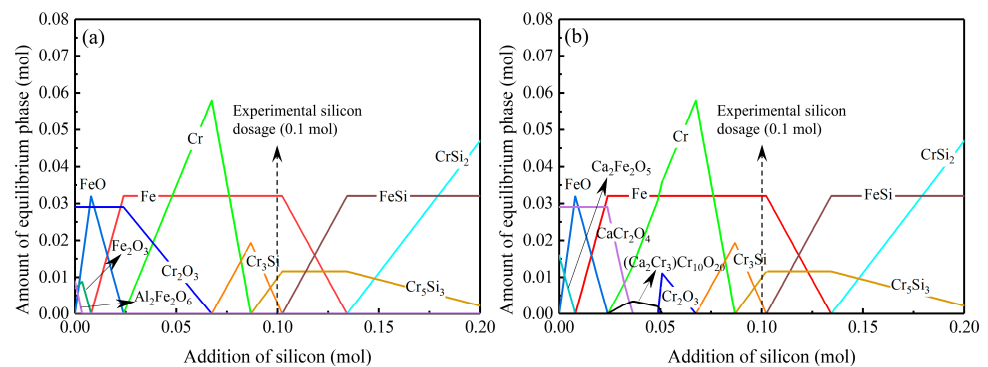
Figure 6. Equilibrium contents of oxides and metals of silicothermic self-reduction compacts as a function of Si addition at 1600 °C: (**a**) without Al_2O_3, CaO addition; (**b**) with Al_2O_3, CaO addition.

3.2. Analysis of the Results of Direct Alloying

Figure 7 illustrates the variation in Cr and Si content over time in samples collected during the direct alloying process using silicothermic self-reduction compacts with and without CaO and Al_2O_3 addition. In the experiment, the masses of chromite ore and Si-containing solid waste in the compacts, as well as the mass of steel, are identical. From the graph, it is evident that the use of Si-containing solid waste as a reducing agent effectively facilitates the reduction of Cr from chromite ore.
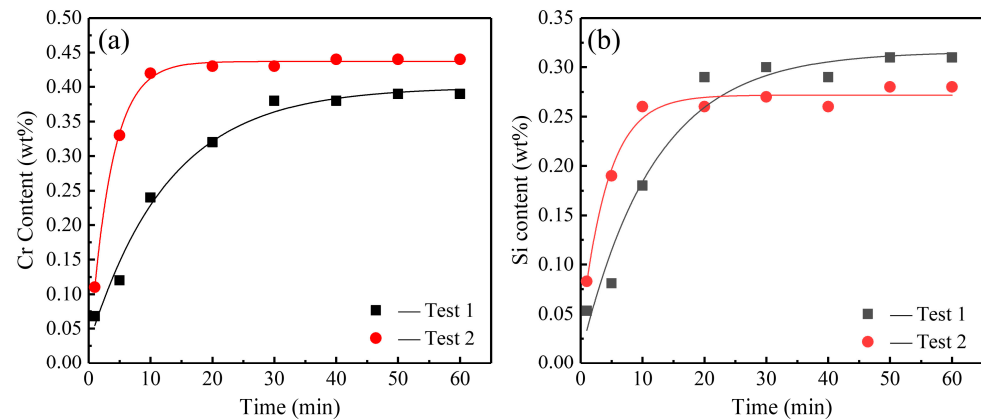
Figure 7. Measured Cr and Si content in melt with time: (**a**) Cr content; (**b**) Si content.

In Test 2, the Cr and Si content stabilizes after 10 min of introducing silicothermic self-reduction compacts into the melt, whereas in Test 1, it takes 20 to 30 min to reach a plateau. This indicates that the rate of Cr reduction in the direct alloying process is faster with silicothermic self-reduction compacts with CaO and Al_2O_3 addition compared to those without CaO and Al_2O_3 addition. Additionally, the Cr content measured in Test 2 is consistently higher than that in Test 1, while the final Si content is lower in Test 2. This implies that silicothermic self-reduction compacts with CaO and Al_2O_3 addition achieve a higher Cr recovery rate, with the final recovery rates for Cr being 95.4% and 86.4% for with CaO and Al_2O_3 addition and without CaO and Al_2O_3 addition self-reduction compacts, respectively. Clearly, the addition of CaO and Al_2O_3 enhances the reduction rate of Cr oxide in chromite ore, thereby increasing the recovery rate of metallic Cr. This observation aligns with previous research findings [27–31].

The direct alloying process of Cr comprises two consecutive steps: (a) the reduction of chromite ore and (b) the diffusion of Fe and Cr into the molten steel [30]. Step (a) can be achieved under appropriate thermodynamic and kinetic conditions. Firstly, based on the thermodynamic analysis results, the reduction reactions of Fe_2O_3 and Cr_2O_3 by Si exhibit relatively low ΔG^0, confirming the feasibility of using silicothermic self-reduction for chromite ore. CaO and Al_2O_3, by reducing the activity of the reduction product SiO_2, decrease the ΔG^0 of the reduction reaction of Cr_2O_3, making it more favorable for the reduction of chromite ore. Secondly, from a kinetic perspective, favorable kinetic conditions not only promote the reduction of chromite ore but also accelerate the diffusion of Fe and Cr. Studies by Takamitsu and Tsomondo [28,29,32] suggest that the reduction of chromite ore and the transfer of metals are controlled by the diffusion of the furnace slag. Under conditions of sufficiently high temperature and a long enough reduction time, obtaining a final liquid slag with low viscosity and good wetting is crucial to ensuring a high Cr recovery rate. Therefore, adjusting the composition of the furnace slag is necessary. This is primarily achieved by adding a certain amount of CaO and Al_2O_3 to the mixture to lower the melting point and viscosity of the slag. This adjustment enhances the diffusion rate of the reducing agent, oxides, and reduction products in the slag, creating favorable kinetic conditions for the reduction of chromite ore [30].

However, the inevitable dissolution of the MgO crucible in the slag occurs. Figure 8 shows images of samples after reduction in Tests 1~3, as well as XRD and SEM-EDS spectrum analysis of the final slag. From the figures, it is evident that the phases in the final slag of Test 1 and Test 2 both include forsterite (Mg_2SiO_4) and spinel ($MgAl_2O_4$), indicating that the slag is saturated with respect to Al_2O_3, MgO, and SiO_2. This implies that a portion of the MgO crucible has dissolved in the slag. In Test 1, the primary phase in the final slag is Mg_2SiO_4, while in Test 2 with added Al_2O_3 and CaO, the major phases in the final slag are $MgAl_2O_4$ and $CaMgSiO_4$.
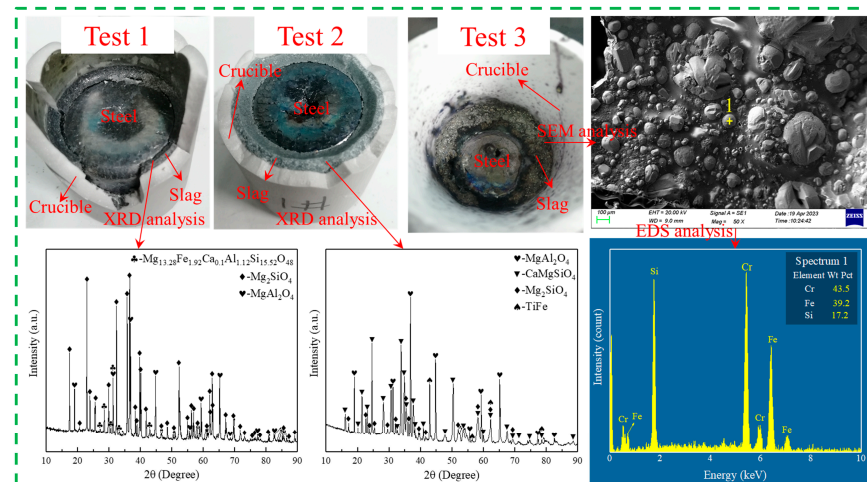
Figure 8. Images of samples after reduction and XRD, SEM-EDS analysis of final slag.

Additionally, Test 3 reveals that after the introduction of silicothermic self-reduction compacts into the crucible, rapid reactions occur, and metallic Cr is almost completely reduced from the chromite ore. It forms an approximately spherical Cr-Fe-Si alloy, with Si and Fe. Since the power is immediately turned off after the introduction of silicothermic self-reduction compacts, causing rapid cooling of the molten steel and slag, deteriorating the metal transfer conditions, the reduced Fe and Cr remain in the slag without sufficient diffusion into the molten steel. Therefore, it can be concluded that the direct alloying process of Cr is controlled by the diffusion of metals in the slag.

Figure 9 displays the morphology of the final slag observed under backscattered electron (BSE) mode in scanning electron microscopy (SEM), along with the corresponding EDS elemental distribution maps. By observing the boundary of the final slag and crucible of Test 1 and Test 2, from a microscopic point of view, the dissolution of the MgO crucible to the slag is clear, and after one hour of holding, the crucible has eroded and there are a lot of small cracks, but from the macroscopic photos (Figure 8), the boundary of the slag and crucible is obvious, and erosion and cracks of the crucible are not clearly observed. The chemical distribution map of the Mg element indicates that Mg is distributed in almost all slag phases, corresponding to the XRD results mentioned earlier, where major phases contain Mg. In Test 3, the elemental distribution maps of Cr and Fe almost overlap, indicating that both elements coexist after reduction and form a Cr-Fe-Si alloy with Si. The chemical distribution map of the Si element also reveals unreacted elemental Si (bright yellow region). Compared to Test 1 and Test 2, the MgO content in the final slag of Test 3 is lower, with MgO percentages of 37.79%, 27.52%, and 3.5% based on XRF chemical composition analysis. This suggests that in Test 3, the dissolution of the MgO crucible into the slag is a relatively slow process, as evidenced by the lower MgO content in the final slag.

However, in previous studies, it was suggested that the dissolution of the MgO crucible increases the viscosity of the furnace slag, deteriorating the reduction kinetics and, therefore, adversely affecting the reduction of Cr_2O_3 [31,33]. Clearly, the dissolution of the MgO crucible in the slag can influence the physicochemical properties of the slag, thereby affecting the reduction of chromite ore. To investigate the impact of the dissolution of the MgO crucible on the melting point and viscosity of the slag in Test 1 and Test 2, phase diagrams of Al_2O_3-MgO-SiO_2 and Al2O3-MgO-SiO_2-20 pct CaO within the temperature range of 1200 to 1800 °C were plotted using the "Phase Diagram" module of FactSage 8.2 software with the "FToxid" database. Additionally, viscosity calculations for selected compositions at the experimental temperature of 1600 °C were simulated using the "Viscosity" module with the "Melt" database, as depicted in Figure 10. The viscosity of the

solid–liquid mixture (oxides that make up the slag, such as CaO, SiO$_2$, Al$_2$O$_3$, and MgO) was approximately calculated based on the Einstein–Roscoe formula [34]:

$$Viscosity_{\text{(solid+liquid mixture)}} \approx Viscosity_{\text{(liquid)}} \times (1 - solid\ fraction)^{-2.5} \qquad (2)$$

where $Viscosity_{\text{(solid+liquid mixture)}}$ is the viscosity of the solid–liquid mixture; $Viscosity_{\text{(liquid)}}$ is the viscosity of the liquid phase, calculated directly from the composition of the liquid slag using the "Viscosity" module with the "Melt" database; and *solid fraction* is the volume fraction of solids in the mixture (solid oxides present in the slag). Due to technical difficulties, few studies have been conducted to experimentally determine the volume fraction of the solid phase in the slag. To simplify the calculations, FactSage calculations can be performed using mass fraction instead of volume fraction to understand the trend of viscosity at different MgO contents [35]. The mass fraction of solids in the mixture is also calculated using the "Equilib" module.
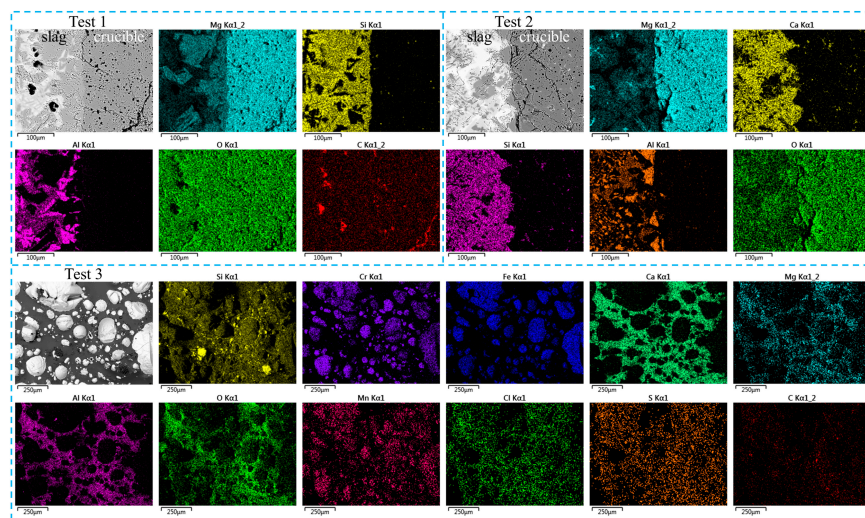

Figure 9. The BSE images of the final slag along with the EDS elemental distribution maps.
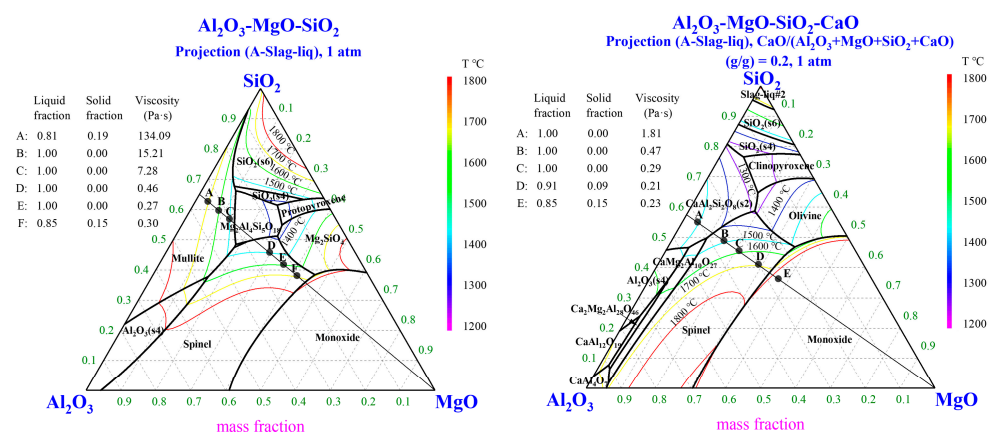

Figure 10. Liquidus isotherm projection and phase diagram of the Al$_2$O$_3$-MgO-SiO$_2$ and Al$_2$O$_3$-MgO-SiO$_2$-20 pct CaO system, and viscosity of different slag phases at 1600 °C.

As mentioned earlier, rapid reactions occur when silicothermic self-reduction compacts are introduced into the crucible, assuming that the reaction has reached its limit, i.e., the mass of SiO$_2$ in the slag remains constant. This can be confirmed through Figure 9, where in Test 3, Cr and Fe elements are concentrated in the alloy, and no significant distribution of Cr and Fe elements is observed in the slag phase. The dissolution of the MgO crucible into the slag is a slow process. Based on the Al$_2$O$_3$ and SiO$_2$ ratios in the final slag, the slag

composition path will follow the black straight line in Figure 10. The composition points for Test 1 and Test 2 final slags are represented by points F and E, respectively.

From the graph, it is evident that the addition of silicothermic self-reduction compacts significantly reduces the melting point of the initial slag (point A). Without the addition of slag, the melting point of the initial slag is 1700 °C, while with the addition of Al_2O_3 and CaO, the melting point of the initial slag drops to 1500 °C. Viscosity calculation results indicate that without CaO and Al_2O_3 addition and with CaO and Al_2O_3 addition, the viscosity at point A at 1600 °C is 134.09 Pa·s and 1.81 Pa·s, respectively. This indicates a significant reduction in the viscosity of the initial slag with the addition of Al_2O_3 and CaO. Without the addition of slag, a large amount of high-melting-point mullite precipitates at point A, resulting in a liquid fraction of only 0.81. Meanwhile, in the liquid composition, the SiO_2 content exceeds 70%, significantly increasing the viscosity of the slag. In contrast, with the addition of Al_2O_3 and CaO, point A is in the low-melting-point calcium feldspar ($CaAl_2Si_2O_{8)}$ phase region. The slag is in a completely liquid state at 1600 °C, with good flowability and low viscosity. This provides favorable kinetic conditions for the reduction of chromite ore and the diffusion of metals, resulting in a faster and more stable reduction of Cr with a higher recovery rate during the direct alloying process (Figure 7).

As the MgO crucible dissolves, the melting points of the two types of slag show different trends. In the Test 1 slag, as the composition point changes from A to C, the dissolved MgO reacts with the existing Al_2O_3 and SiO_2 in the original slag to form a liquid slag, significantly lowering the melting point. Apparently, MgO is a chain-breaker; it breaks silicate chains by creating oxide bridges. With further increases in MgO content, when the composition point reaches D, the slag melting point begins to rise. In Test 2 slag, the increase in MgO content leads to the precipitation of spinel with a higher melting point, causing the slag melting point to increase. The change in slag viscosity does not follow the same trend as the melting point; from the graph, it can be observed that the viscosity of the Al_2O_3-MgO-SiO_2 and Al_2O_3-MgO-SiO_2-20 pct CaO slag systems decreases first and then increases with increasing MgO content.

In other words, the initial dissolution of the MgO crucible reduces the slag viscosity. Unlike the results reported by Hu [31] and Nakao [33], under the experimental conditions of this study, the viscosity of Test 1 and Test 2 slags increases only when the composition points reach E and D, respectively. This means that the viscosity of the slag increases only when the MgO content in the slag exceeds 36% and 29.1% for Test 1 and Test 2, respectively.

In conclusion, the addition of Al_2O_3 and CaO can significantly reduce the melting point and viscosity of the initial slag, thereby promoting the reduction of chromite ore. Although the dissolution of the MgO crucible can lower the melting point and viscosity of the early slag, its dissolution is a relatively slow process compared to the rapid silicothermic self-reduction reaction. During the rapid reduction phase, the reduction of chromite ore has already reached its limit. Therefore, the Cr recovery rate depends on the composition of the initial slag after rapid reduction. When chromite spinel particles enter the slag, their chances of encountering a reducing agent are immediately minimized, leading to the interruption of the final reduction. The reduction of chromite ore in the slag is limited, and consequently, Cr losses in the slag are inevitable [36].

3.3. The Mechanism of Silicothermic Self-Reduction

Figure 11 illustrates the schematic diagram of the silicothermic self-reduction reaction mechanism. Thermodynamic analysis indicates that Fe_2O_3 is initially reduced to FeO, which is then further reduced to metallic Fe. The reduction of Cr_2O_3, however, commences only after the reduction of Fe oxides. Previous studies suggest that the reduction kinetics of Fe oxides in chromite spinel are more favorable than those of Cr oxides. Theoretically, when Si is employed as a reducing agent, the reduction of Fe_2O_3 to FeO occurs between 600 and 750 °C, with the temperature range of 750 to 900 °C for the conversion of FeO to metallic Fe. However, the reduction rate is relatively low at lower temperatures, and the complete transformation of Fe_2O_3 to Fe necessitates temperatures ranging from 1100 to

1300 °C, approximately reaching 1300 °C for the conversion of Cr_2O_3 to metallic Cr [36,37]. As shown in Figure 11a, the self-reduction compacts are first added to the surface of the molten steel, and as the temperature reaches the reduction temperature of iron oxides, a direct reduction reaction is initiated at the interface between chromite ore and Si, and Fe_2O_3 is reduced to FeO (Figure 11b). The temperature continues to increase, as shown in Figure 11c, and metallic Fe is first reduced, at which point the reduced Fe forms a low-melting-point Fe-Si alloy with unreacted Si. As the temperature is further increased to the Cr_2O_3 reduction temperature, the metallic Cr is reduced, and the newly formed Cr can be rapidly dissolved into the Fe-Si alloy, creating a Cr-Fe-Si alloy melt enriched in both Fe and Cr (Figure 11d). Figure 12 illustrates the liquidus isotherm projection phase diagram of the Cr-Si-Fe system, along with the EDS compositional analysis of the reduced Cr-Fe-Si alloy observed in Test 3. From the figure, it is evident that the temperatures during the reduction process and the composition of the final alloy lie below 1400 °C in the liquidus region. Therefore, at the steelmaking temperature of 1600 °C, the reduced alloy exists in a liquid state, facilitating the aggregation and growth of metallic droplets. Ultimately, the reduced Cr and Fe diffuse into the steel from the slag, achieving the direct alloying of Cr.
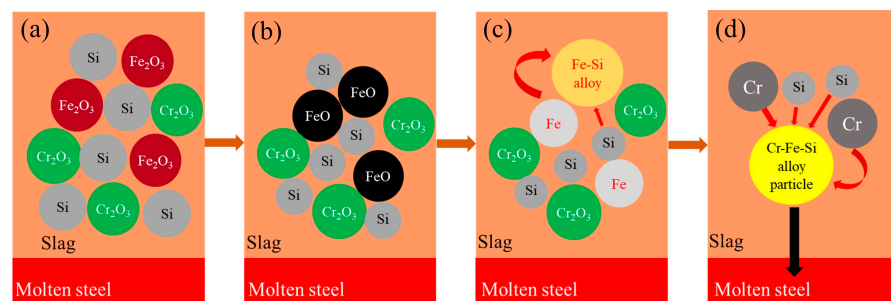
Figure 11. Schematic diagram of silicothermic self-reduction mechanism. (**a**) Adding the self-reduction compact to molten steel; (**b**) Reduction of Fe_2O_3 to FeO; (**c**) Reduction of FeO to Fe and production of Fe-Si alloy; (**d**) Reduction of Cr_2O_3 to Cr and production and diffusion of Cr-Fe-Si alloy.
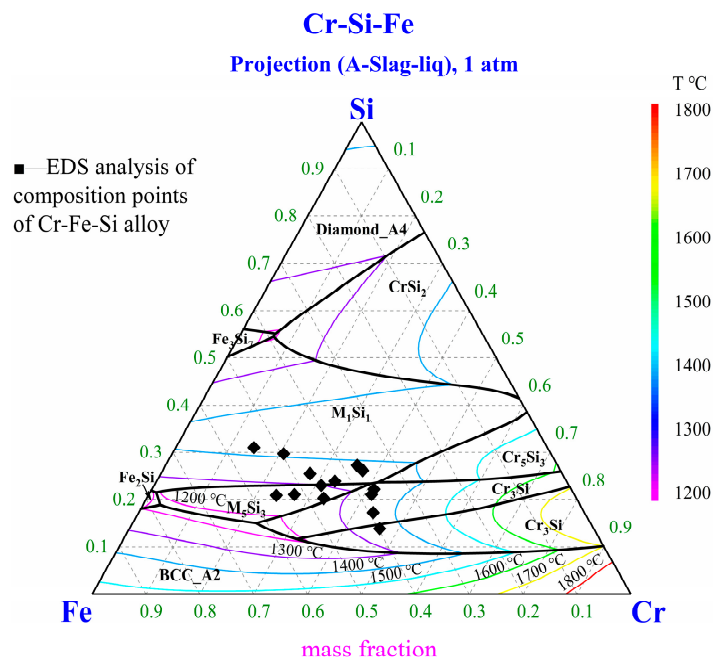
Figure 12. Liquidus isotherm projection and phase diagram of the Fe-Si-Cr system.

Indeed, the presence of Fe serves to facilitate the reduction of Cr_2O_3, and the Fe derived from chromite ore exhibits analogous effects. This phenomenon has been corroborated by

other investigators who examined the impact of varying Fe-to-Cr ratios on the reduction of chromite ore. Their findings affirm that chromite ores with elevated total Fe contents undergo reduction at an accelerated pace, yielding a higher Cr recovery [25,38]. This can be chiefly ascribed to the existence of a molten alloy. On the one hand, a profusion of Fe-Si alloy droplets emerges prior to the reduction of Cr_2O_3. These droplets, formed through the dissolution of Cr liberated during reduction, serve to diminish the thermodynamic activity of newly reduced Cr in chromite ore. This reduction proves advantageous in lowering the ΔG^0 of the reaction, thereby expediting the swift reduction of Cr. On the other hand, an excess of metallic Si exerts its influence by fostering the formation of low-melting-point phases such as Cr-Si or Cr-Fe-Si (refer to Figure 12), thereby attenuating the activity of Cr in the Cr-Fe-Si alloy. This sustained reduction in Cr activity, in turn, serves to propel the reduction process, enhancing its overall efficacy.

4. Conclusions

1. Within chromite ore, Fe_2O_3 is preferentially reduced by Si over Cr_2O_3. The introduction of CaO and Al_2O_3 serves to alter the equilibrium states of Fe and Cr oxides, concurrently diminishing the activity of the reduction product SiO_2. This leads to a conspicuous reduction in the ΔG^0 of the reduction reaction.

2. The addition of CaO and Al_2O_3 significantly lowers the melting point and viscosity of the initial slag. The melting point and viscosity of the initial slag, originally 1700 °C and 134.09 Pa·s without additives, are markedly decreased to 1500 °C and 1.81 Pa·s, respectively, upon the addition of slag.

3. The incorporation of CaO and Al_2O_3 expedites the reduction of Cr and enhances the Cr recovery rate. The final recovery rates of Cr in the silicothermic self-reduction compacts, with and without CaO and Al_2O_3 addition, directly alloying the molten steel, are 95.4% and 86.4%, respectively. Therefore, employing Si-containing solid waste as a reductant for the direct reduction and alloying of chromite ore is deemed viable. This not only addresses the environmental pollution and resource wastage resulting from Si-containing solid waste but also transforms it into a valuable resource, concurrently reducing the cost associated with Cr alloying in molten steel. However, to achieve the goal of the efficient and economical direct reduction alloying of chromium oxide, the optimum reductant ratio and the different $w(CaO)/w(Al_2O_3)$ ratio, as well as the amount of CaO and Al_2O_3 additions, still need to be further investigated.

4. However, a side-effect of steel alloying by silicothermic self-reduction is that the reduction product SiO_2 reduces the basicity in the LF refining furnace, and in practice, it is necessary to supplement the LF furnace with activated lime to ensure that the basicity remains unchanged. In addition, to achieve higher metal yields, excess reductant Si must be added, which results in the introduction of additional Si into the steel, a factor that needs to be taken into account when deoxidizing or alloying with ferrosilicon. In terms of industrial relevance, the steel industry can provide for the consumption of Si-containing solid waste generated by the silicone industry. Silicothermic self-reduction direct alloying steelmaking is useful for the smelting of ultra-low carbon steels, such as 301L (12Cr17Ni7) stainless steel, to avoid the carbon increase in steel due to the introduction of carbon from high-carbon ferrochromium.

Conflicts of Interest: The authors declare no conflicts of interest.

References

1. Zhao, L.; Li, Z.; Xi, F.; Li, S.; Ma, W.; Wu, J.; Wei, K. Purification of Organosilicon Waste Silicon Powder with Hydrometallurgy. *Metals* **2023**, *13*, 950. [CrossRef]
2. Zhang, P.; Zhang, D.; Dong, J.; Chen, G.; Li, J. Direct Synthesis of Methylchlorosilanes: Catalysts, Mechanisms, Reaction Conditions, and Reactor Designs. *Org. Process Res. Dev.* **2022**, *26*, 2270–2280. [CrossRef]
3. Xie, J.; Hu, Y.; Gao, Y.; Sun, F. Synthesis and Properties of Trifluoromethyl Organosilicon Cycloaliphatic Epoxy Monomers for Cationic Photopolymerization. *J. Appl. Polym. Sci.* **2023**, *140*, e53987. [CrossRef]
4. Bezlepkina, K.; Belikova, I.; Aristova, V.; Klokova, K.; Ardabevskaia, S.; Pereyaslavtsev, A.; Migulin, D.; Milenin, S. Optimized Synthesis of Functional Organosilicon Monomers and Polymers Exploiting New Types of CuAAC Recoverable Heterogeneous Catalysts. *React. Chem. Eng.* **2024**. Advance Article. [CrossRef]
5. Yuan, M.; Lu, X.; Ma, X.; Lin, H.; Lu, A.; Shao, L.; Xin, Z. Polybenzoxazine/Organosilicon Composites with Low Dielectric Constant and Dielectric Loss. *Chin. J. Chem. Eng.* **2023**, *64*, 241–249. [CrossRef]
6. Hamawand, I.B.; Hanna, F.Z.; Jalhoom, M.G. Production of Organosilane by The Direct Reaction of Silicon with Methyl Chloride. *Eng. Technol.* **2007**, *25*, 1128–1142. [CrossRef]
7. Zhang, Y.; Li, J.; Liu, H.; Ji, Y.; Zhong, Z.; Su, F. Recent Advances in Rochow-Müller Process Research: Driving to Molecular Catalysis and to A More Sustainable Silicone Industry. *ChemCatChem* **2019**, *11*, 2757–2779. [CrossRef]
8. Blaser, E.; Rosier, C.; Huet, M.; Geantet, C.; Loridant, S. Catalytic Cracking of CH_3Cl on Copper-Based Phases. *Catal. Sci. Technol.* **2022**, *12*, 2006–2014. [CrossRef]
9. Zhang, N.; Xiong, Y.; Zhao, J. Conversion of a Direct Process High-Boiling Residue to Monosilanes by a Two-Step Catalysis Approach. *Res. Chem. Intermed.* **2007**, *33*, 613–622. [CrossRef]
10. Wang, G.; Ye, Z.; Dong, S.; Wang, J. Harmless Process of Organic Matter in Organosilicon Waste Residue by Fluidization-like DDBD Reactor: Temperature Action and Mechanism. *Chemosphere* **2023**, *322*, 138116. [CrossRef]
11. Wang, A.; Jiang, Y.; Chen, W.; Yin, H.; Liu, Y.; Shen, Y.; Jiang, T.; Wu, Z. [BMIM]Cl-nAlCl$_3$ Ionic Liquid-Catalyzed Redistribution Reaction between Methyltrichlorosilane and Low-Boiling Residue to Dimethyldichlorosilane. *J. Ind. Eng. Chem.* **2012**, *18*, 237–242. [CrossRef]
12. Yu, J.; Zhan, H.; Wang, Y.; Zhang, Z.; Chen, H.; Li, H.; Zhong, Z.; Su, F. Graphite Microspheres Decorated with Si Particles Derived from Waste Solid of Organosilane Industry as High Capacity Anodes for Li-Ion Batteries. *J. Power Sources* **2013**, *228*, 112–119. [CrossRef]
13. Lu, X.; Gu, F.; Liu, Q.; Gao, J.; Jia, L.; Xu, G.; Zhong, Z.; Su, F. Ni–MnO$_x$ Catalysts Supported on Al$_2$O$_3$-Modified Si Waste with Outstanding CO Methanation Catalytic Performance. *Ind. Eng. Chem. Res.* **2015**, *54*, 12516–12524. [CrossRef]
14. Liu, H.; Ji, Y.; Zhu, Y.; Wang, G.; Wang, X.; Zhong, Z.; Su, F. Converting Industrial Waste Contact Masses into Effective Multicomponent Copper-Based Catalysts for the Rochow Process. *Particuology* **2018**, *37*, 1–8. [CrossRef]
15. Guo, X.; Zhang, Z.; Xing, P.; Wang, S.; Guo, Y.; Zhuang, Y. Kinetic Mechanism of Copper Extraction from Methylchlorosilane Slurry Residue Using Hydrogen Peroxide as Oxidant. *Chin. J. Chem. Eng.* **2023**, *60*, 228–234. [CrossRef]
16. Cai, X.; Wu, J.; Wei, K.; Ma, W. Study on the Purification Process of Waste Silicon Powder in the Synthesis Process of Organosilicon Monomer. *Silicon* **2023**. [CrossRef]
17. Salina, V.; Zayakin, O.; Zhuchkov, V. Thermodynamic Simulation of the Silicothermic Reduction of Chromium Ore Elements. *Russ. Metall.* **2020**, *2020*, 14–20. [CrossRef]
18. Salina, V.; Zhuchkov, V.; Zayakin, O. Thermodynamic Simulation of Silicothermic Reduction of Chromium. *Steel Transl.* **2020**, *50*, 84–89. [CrossRef]
19. Salina, V.; Zhuchkov, V.; Zayakin, O. A Study of Nickel and Iron Reduction Silicothermic Process by Thermodynamic Simulation. *MSF* **2020**, *989*, 511–516. [CrossRef]
20. Heo, J.; Chung, Y.; Park, J. Effect of CaF$_2$ Addition on the Silicothermic Reduction of MnO in Ferromanganese Slag. *Metall. Mater. Trans. B* **2015**, *46*, 1154–1161. [CrossRef]
21. Heo, J.; Park, J. Manganese Recovery by Silicothermic Reduction of MnO in BaO-MnO-MgO-CaF$_2$ (-SiO$_2$) Slags. *Metall. Mater. Trans. B* **2018**, *49*, 514–518. [CrossRef]
22. Lenaz, D.; Braidotti, R.; Princivalle, F.; Garuti, G.; Zaccarini, F. Crystal Chemistry and Structural Refinement of Chromites from Different Chromitite Layers and Xenoliths of the Bushveld Complex. *Eur. J. Miner.* **2007**, *19*, 599–609. [CrossRef]
23. Zhang, Y.; Ji, Y.; Li, J.; Liu, H.; Zhong, Z.; Su, F. Hierarchical Zinc-Copper Oxide Hollow Microspheres as Active Rochow Reaction Catalysts: The Formation and Effect of Charge Transferable Interfaces. *J. Catal.* **2017**, *348*, 233–245. [CrossRef]
24. He, Q.; Yu, J.; Wang, Y.; Zhong, Z.; Jiang, J.; Su, F. Silicon Nanoparticles Prepared from Industrial Wastes as High-Performing Anode Materials for Lithium Ion Batteries. *Solid. State Ionics* **2018**, *325*, 141–147. [CrossRef]
25. Hu, X.; Yang, Q.; Ökvist, L.S.; Björkman, B. Thermal Analysis Study on the Carbothermic Reduction of Chromite Ore with the Addition of Mill Scale. *Steel Res. Int.* **2016**, *87*, 562–570. [CrossRef]
26. Zhu, H.; Li, Z.; Yang, H.; Luo, L. Carbothermic Reduction of MoO$_3$ for Direct Alloying Process. *J. Iron Steel Res. Int.* **2013**, *20*, 51–56. [CrossRef]

27. Ding, Y.; Warner, N. Catalytic Reduction of Carbon-Chromite Composite Pellets by Lime. *Thermochim. Acta* **1997**, *292*, 85–94. [CrossRef]

28. Nakasuga, T.; Sun, H.; Nakashima, K.; Mori, K. Reduction Rate of Cr_2O_3 in a Solid Powder State and in CaO-SiO_2-Al_2O_3-CaF_2 Slags by Fe-C-Si Melts. *ISIJ Int.* **2001**, *41*, 937–944. [CrossRef]

29. Nakasuga, T.; Nakashima, K.; Mori, K. Recovery Rate of Chromium from Stainless Slag by Iron Melts. *ISIJ Int.* **2004**, *44*, 665–672. [CrossRef]

30. Hu, X.; Wang, H.; Teng, L.; Seetharaman, S. Direct Chromium Alloying by Chromite Ore with the Presence of Metallic Iron. *J. Min. Metall. Sect. B* **2013**, *49*, 207–215. [CrossRef]

31. Hu, X.; Ökvist, L.S.; Eriksson, J.; Yang, Q.; Björkman, B. Direct Alloying Steel with Chromium by Briquettes Made from Chromite Ore, Mill Scale, and Petroleum Coke. *Steel Res. Int.* **2017**, *88*, 1600247. [CrossRef]

32. Tsomondo, M.B.C.; Simbi, D.J. Kinetics of Chromite Ore Reduction from MgO-CaO-SiO_2-FeO-Cr_2O_3-Al_2O_3 Slag System by Carbon Dissolved in High Carbon Ferrochromium Alloy Bath. *Ironmak. Steelmak.* **2002**, *29*, 22–28. [CrossRef]

33. Nakao, R.; Tanaka, S.; Takano, H. Effect of Slag on Decarburization Reaction of Stainless Steel Melt. *Tetsu-to-Hagane* **1994**, *80*, 30–35. [CrossRef] [PubMed]

34. Seok, S.H.; Jung, S.M.; Lee, Y.S.; Dongjoon, M. Viscosity of Highly Basic Slags. *ISIJ Int.* **2007**, *47*, 1090–1096. [CrossRef]

35. Li, F.; Liu, X.; Zhao, C.; Yang, Z.; Fan, H.; Han, G.; Xu, M.; Wang, Z.; Fang, Y. Effects of Sludge on the Ash Fusion Behaviors of High Ash-Fusion-Temperature Coal and Its Ash Viscosity Predication. *J. Energy Inst.* **2023**, *108*, 101254. [CrossRef]

36. XU, S.; DAI, W. The Melting Behaviour of Chromite Ores and the Formation of Slag in the Production of High-Carbon Ferrochromium. In Proceedings of the 6th International Ferroalloys Congress (INFACON 6), SAIMM, Cape Town, South Africa, 8–11 March 1992; pp. 87–92.

37. Hu, T.; Dai, L.; Guo, Q.; Liu, B.; Gui, Q.; Gang, R.; Ji, H.; Zhang, L. Dielectric Properties of Silicothermic Reduction Chromite in the Microwave Field. *ACS Omega* **2020**, *5*, 12672–12681. [CrossRef]

38. Nafziger, R.H.; Tress, J.E.; Paige, J.I. Carbothermic Reduction of Domestic Chromites. *Metall. Trans. B* **1979**, *10*, 5–14. [CrossRef]